

# Kagome Lattice from Exciton-Polariton Prospective

D. R. Gulevich,<sup>1,\*</sup> D. Yudin,<sup>1,2</sup> I. V. Iorsh,<sup>1,2</sup> and I. A. Shelykh<sup>1,2,3</sup>

<sup>1</sup>*ITMO University, St. Petersburg 197101, Russia*

<sup>2</sup>*Division of Physics and Applied Physics, Nanyang Technological University 637371, Singapore*

<sup>3</sup>*Science Institute, University of Iceland, Dunhagi 3, IS-107, Reykjavik, Iceland*

(Dated: July 19, 2022)

We study a system of microcavity pillars arranged into kagome lattice. We show that polarization-dependent tunnel coupling of microcavity pillars leads to the emergence of the effective spin-orbit interaction consisting of the Dresselhaus and Rashba terms, similar to the case of polaritonic graphene studied earlier. Appearance of the effective spin-orbit interaction combined with the time-reversal symmetry-breaking resulting from the application of the magnetic field leads to the nontrivial topological properties of the Bloch bundles of polaritonic wavefunction. These are manifested in opening of the gap in the band structure and topological edge states localized on the boundary. Such states are analogs of the edge states arising in topological insulators and therefore present one more example of polaritonic system serving as analogue quantum simulator of condensed matter phases. Our study of polarization properties of the edge states clearly demonstrate that opening of the gap is associated with the band inversion in the region of the Dirac points of the Brillouin zone where the two bands corresponding to polaritons of opposite polarization meet. For one particular type of boundary we observe a non-monotonous energy dispersion of the edge state which allows existence of the additional pair of edge states in a certain interval of energies inside the gap.

## I. INTRODUCTION

The modern theory of phase transitions originates from the suggestion of Landau that the transition from one state of matter to another must correspond to a spontaneous symmetry breaking<sup>1</sup>. This idea gives rise to the phenomenological theory of phase transitions which is formulated in terms of the order parameter. Quantum Hall effect (QHE)<sup>2</sup>, discovered more than 30 years ago, has posed some awkward questions regarding the original Landau approach. Indeed, the state of electrons in QHE might be treated as a phase since the macroscopic observables such as the quantized Hall conductivity are not affected by smooth variations of material parameters. Still the transitions between different Hall plateaus are not related to violation of any underlying symmetry<sup>3</sup>.

The puzzle has been successfully resolved by introduction of the concept of topological order<sup>4</sup>. The quasiclassical dynamics of the wave packet propagating in periodic dissipative media turned out to be instrumental for the theoretical understanding of this type of order. In an attempt to explain the anomalous Hall effect in a ferromagnet as an intrinsic property of the band structure, Karplus and Luttinger<sup>5</sup> pointed out that the position operator in a periodic lattice fails to commute with itself. As a consequence the standard quasiclassical expression for the group velocity acquires an anomalous term, which is proportional to what is now called Berry curvature<sup>6</sup>. Being integrated over a Brillouin zone the Berry curvature gives topological invariant known as Chern number. The system possessing a non-zero topological invariant may be called topological matter<sup>7</sup>.

Observation of the spin Hall effect in a class of semiconductors with strong spin-orbit coupling<sup>8–11</sup> has revived an interest to topological phases of matter. A term topological insulator has been coined to describe a sys-

tem which behaves like an insulator in the bulk but has conducting surface. The conduction is due to the presence of the edge states which possess remarkable property of topological protection. It is predicted that electrons traveling along the surface are protected against backscattering and preserve their phase coherence over long distances despite the presence of impurities, interactions, and external fields.

It has been recently realized that topologically non-trivial phases may arise not only in the condensed matter electronic systems but also in photonic structures<sup>12,13</sup>. The artificial gauge fields in photonic structures can be realized in a system with periodic variation of dielectric permittivity. Large wavelength and coherence length of photons makes it simpler to realize diverse non-trivial landscapes of photonic nanostructures as compared to the electronic counterparts. At the same time, magnetic field control of the topological properties in photonic structures is precluded at optical frequencies because of the lack of natural magnetic materials in the optical frequency range (certain realizations of ferromagnetic photonic crystals for microwave region have been proposed in Ref. 14).

Thus, it would be favourable to consider the system which would allow flexible control over the topological properties both via the external magnetic fields and the periodic potentials. Exciton-polaritons, quasi-particles originating due to the strong-light matter coupling between the quantum well excitons and cavity photons<sup>15</sup> are good candidates. Exciton-polaritons attract significant interest for the last two decades because of the opportunities they offer for the observation of a wide class of quantum collective phenomena ranging from BEC and superfluidity<sup>16,17</sup> to polaritonic lasing<sup>18,19</sup> at high temperatures. Due to the hybrid light-matter nature, exciton-polaritons can be controlled both with ex-

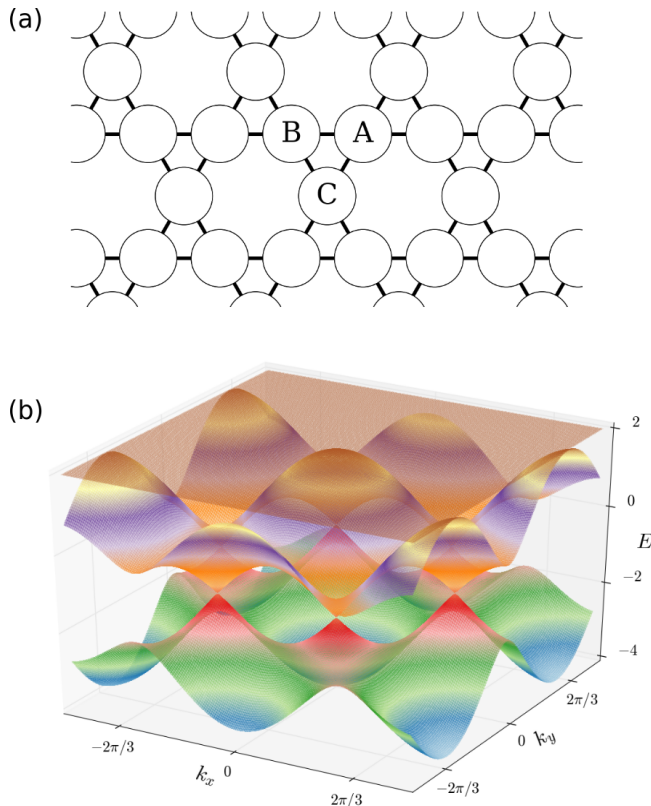


FIG. 1. (a) Sketch of two-dimensional kagome lattice formed by coupled microcavity pillars. Labels  $A$ ,  $B$ ,  $C$  mark three inequivalent sites of the unit cell. (b) Band structure of the kagome lattice in the absence of magnetic field ( $\Omega = 0$ ) and TE-TM splitting ( $\delta J = 0$ ).

ternal magnetic field since it creates Zeeman splitting for the excitonic component and structure patterning which forms periodic potential for the photonic part. Various techniques were proposed for creation of the potential landscapes for polaritons. They include surface acoustic waves<sup>20,21</sup>, metal deposition<sup>22–25</sup> and beam lithography and etching of the sample producing lattices of coupled micropillars<sup>26,27</sup>. Moreover, polaritonic system exhibit analogs of spin-orbit interaction<sup>28,29</sup> stemming from the splitting between TE and TM photonic modes<sup>30–32</sup>.

Recently there have been several proposals to simulate topological phases of condensed matter systems with polaritons<sup>33–35</sup>. For this, one needs to identify the systems with time-reversal and inversion symmetric band structure characterized by the touching bands which split as soon as the time-reversal symmetry is broken. The boundary between topological phases with different Chern numbers (or other topological invariants) must support edge modes which are topologically protected against variations of the material parameters unless the band gap in the bulk of the material is collapsed. Such modes are analogs of the edge states arising on a surface of two-dimensional topological insulators and

therefore polaritonic systems can play a useful role of a simulator to study topological order in a well-controlled experimental environment. In this paper we consider in details one particular example with high experimental relevance, namely the kagome lattice of polariton pillars.

The paper is organized as follows. In Section II we introduce the model of polaritonic kagome lattice. We demonstrate the appearance of energy gaps when time-reversal and inversion symmetries are broken by magnetic field and TE-TM splitting. In Section III we study topological properties of the Bloch band bundles for polariton states in kagome lattice. Section IV is devoted to study of edge modes which arise due to non-trivial topology of the Bloch bands, paying particular attention to their localization and polarization properties.

## II. BAND STRUCTURE OF POLARITON KAGOME LATTICE

We consider exciton-polariton microcavity pillars connected by tunnel coupling and arranged into a kagome lattice as shown in Fig. 1a. Kagome lattice<sup>36</sup>, has a high degree of frustration compared to other 2D lattices, e.g. triangular and square lattices. In the magnetism community it was very recently proposed as a candidate for magnetic material possessing quasiparticles with topological properties<sup>37,38</sup>. In the tight-binding approximation with nearest-neighbor (NN) coupling  $-J < 0$  the highest energy band of kagome lattice band structure is completely flat while the lower bands touch at Dirac points in the corners of hexagonal Brillouin zone, see Fig. 1a and b.

When TE-TM splitting is present in the junction connecting the two pillars, the linear polarization modes in neighboring pillars experience different tunnel barriers<sup>28,29,33</sup>. If  $|L_j\rangle, |T_j\rangle$  are states of linear polarizations directed along and transverse to the direction connecting the centers of two neighbouring pillars  $j = 1, 2$ , then  $\langle L_1 | \hat{V} | L_2 \rangle = -J - \delta J$ ,  $\langle T_1 | \hat{V} | T_2 \rangle = -J + \delta J$  where  $\hat{V}$  is the tunneling operator which links neighbouring pillars and  $2\delta J$  is the difference of the tunnel couplings of linearly polarized exciton-polaritons arising due to the TE-TM splitting. Such polarization-dependent tunneling has been shown to be responsible for appearance of effective spin-orbit interaction in polaritonic benzene molecule<sup>28</sup> and polaritonic graphene<sup>33</sup>. We will show that the polarization-dependent tunneling results in Rashba and Dresselhaus spin-orbit interaction terms in polaritonic kagome lattice and leads to opening of the gap in the vicinity of the Dirac points when time-reversal symmetry of the system is broken by external magnetic field.

In the tight-binding approximation and with account of the polarization dependent coupling, the Hamiltonian

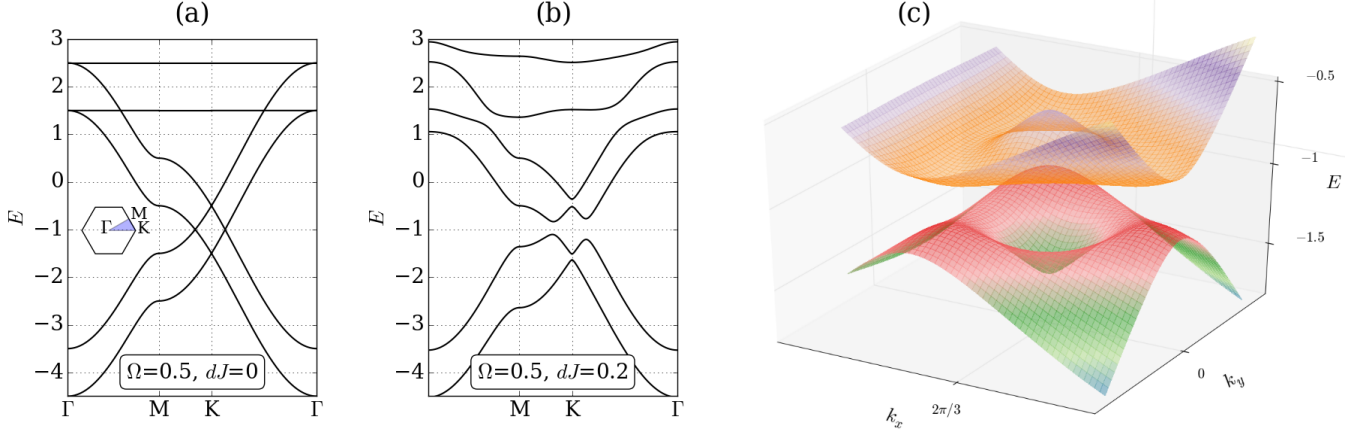


FIG. 2. Mechanism of gap opening in polariton kagome lattice. (a) Gapless band structure at magnetic field  $\Omega = 0.5$  and absence of TE-TM splitting  $\delta J = 0$ . (b) Same magnetic field is applied but a finite TE-TM splitting  $\delta J = 0.2$  is present. (c) Zoom of the band structure in the vicinity of the Dirac point of the Brillouin zone at  $\Omega = 0.5$ ,  $\delta J = 0$ . The two bands just below and above the opened gap are shown.

for polaritons in the basis of circular polarization reads

$$\hat{H} = \Omega \sum_{i,\sigma=\pm} \sigma \hat{a}_{i,\sigma}^\dagger \hat{a}_{i,\sigma} - J \sum_{\langle ij \rangle, \sigma=\pm} \hat{a}_{i,\sigma}^\dagger \hat{a}_{j,\sigma} - \delta J \sum_{\langle ij \rangle} \left( e^{-2i\varphi_{ij}} \hat{a}_{i,+}^\dagger \hat{a}_{j,-} + e^{2i\varphi_{ij}} \hat{a}_{i,-}^\dagger \hat{a}_{j,+} \right) + h.c. \quad (1)$$

Here, the summation  $\langle ij \rangle$  is over nearest neighbors, operators  $\hat{a}_{i,\sigma}^\dagger$  ( $\hat{a}_{i,\sigma}$ ) create (annihilate) exciton-polariton of circular polarization  $\sigma$  at sites  $A, B, C$  of the  $i$ -th unit cell, angles  $\varphi_{ij} \in \{\varphi_{AB}, \varphi_{AC}, \varphi_{BC}\}$  specify directions of vectors connecting sites of the unit cell. The first term in (1) describes the Zeeman energy splitting ( $2\Omega$ ) of the circular polarized components, the second term stands for the NN hopping and the third term is the polarization-dependent coupling of cross-polarized polaritons in neighboring pillars.

The eigenstates of the tight-binding Hamiltonian (1) can be searched in the form of linear combination of the Bloch wavefunctions associated with sublattices  $A, B$  and  $C$ ,

$$|\psi_{\mathbf{k}}\rangle = \sum_{\sigma} \left( A_{\mathbf{k}}^{\sigma} |\psi_{\mathbf{k}}^{A\sigma}\rangle + B_{\mathbf{k}}^{\sigma} |\psi_{\mathbf{k}}^{B\sigma}\rangle + C_{\mathbf{k}}^{\sigma} |\psi_{\mathbf{k}}^{C\sigma}\rangle \right). \quad (2)$$

Here, index  $\sigma$  runs over the two circular polarizations and the Bloch wavefunctions  $|\psi_{\mathbf{k}}^{L\sigma}\rangle$  with  $L = A, B, C$ , are linear superpositions of states  $|\phi_j^{L\sigma}\rangle$  localized on site  $j$ ,

$$|\psi_{\mathbf{k}}^{L\sigma}\rangle = \sum_j e^{-i\mathbf{k}\cdot\mathbf{R}_j^L} |\phi_j^{L\sigma}\rangle. \quad (3)$$

In the basis  $\{|\psi_{\mathbf{k}}^{A+}\rangle, |\psi_{\mathbf{k}}^{A-}\rangle, |\psi_{\mathbf{k}}^{B+}\rangle, |\psi_{\mathbf{k}}^{B-}\rangle, |\psi_{\mathbf{k}}^{C+}\rangle, |\psi_{\mathbf{k}}^{C-}\rangle\}$  the Hamiltonian reads

$$\hat{H}_{\mathbf{k}} = \begin{pmatrix} \Omega\sigma_z & F_{\mathbf{k}}^{AB} & F_{\mathbf{k}}^{AC} \\ F_{\mathbf{k}}^{AB} & \Omega\sigma_z & F_{\mathbf{k}}^{BC} \\ F_{\mathbf{k}}^{AC} & F_{\mathbf{k}}^{BC} & \Omega\sigma_z \end{pmatrix}, \quad (4)$$

where  $\hat{\sigma}_z$  is the Pauli matrix and matrices  $\hat{F}_{\mathbf{k}}^{\mathbf{d}}$  for  $\mathbf{d} = AB, AC, BC$ , are

$$\hat{F}_{\mathbf{k}}^{\mathbf{d}} = -2 \begin{pmatrix} J \cos \mathbf{k} \cdot \mathbf{d} & \delta J e^{-2i\varphi_{\mathbf{d}}} \cos \mathbf{k} \cdot \mathbf{d} \\ \delta J e^{2i\varphi_{\mathbf{d}}} \cos \mathbf{k} \cdot \mathbf{d} & J \cos \mathbf{k} \cdot \mathbf{d} \end{pmatrix}. \quad (5)$$

The eigenstates and eigenenergies are defined by the stationary Schrödinger equation

$$\hat{H}_{\mathbf{k}} u_{\mathbf{k},m} = E_{\mathbf{k},m} u_{\mathbf{k},m}. \quad (6)$$

In what follows we will use normalized units by setting the characteristic length  $|\mathbf{d}|$  and energy  $J$  to unity. In the absence of the magnetic field  $\Omega = 0$  and TE-TM splitting  $\delta J = 0$  the arising band structure coincides with the standard band structure of kagome lattice shown in Figure 1. The presence of a non-zero magnetic field ( $\Omega \neq 0$ ) and TE-TM splitting ( $\delta J \neq 0$ ) break the time reversal and inversion symmetries of the system. This leads to the opening of a band gap at the Dirac points of the Brillouin zone, see Fig. 2a and b. The band structure arising from the gap opening in the vicinity of the Dirac point is shown in Fig. 2c.

To investigate the properties of the system in the vicinity of the gap we perform decomposition near the Dirac point. Projecting to the subspace of eigenstates calculated at  $\delta J = 0$ ,  $\Omega = 0$ , and dropping unimportant additive constant we get the Hamiltonian in the vicinity of the Dirac point  $\mathbf{K}$ ,

$$\hat{H} = \hat{H}_0 + \hat{H}_{\mathbf{q}} + \hat{H}_{\mathbf{q}}^{SO}, \quad (7)$$

where  $\mathbf{q} = \mathbf{k} - \mathbf{K}$  and we explicitly separated  $\mathbf{q}$ -independent and  $\mathbf{q}$ -dependent parts,

$$\hat{H}_0 = \Omega \hat{\sigma}_0 \otimes \hat{\sigma}_z + \frac{\delta J}{2} (\hat{\sigma}_0 - \hat{\sigma}_y) \otimes (\sqrt{3}\hat{\sigma}_x + \hat{\sigma}_y), \quad (8)$$

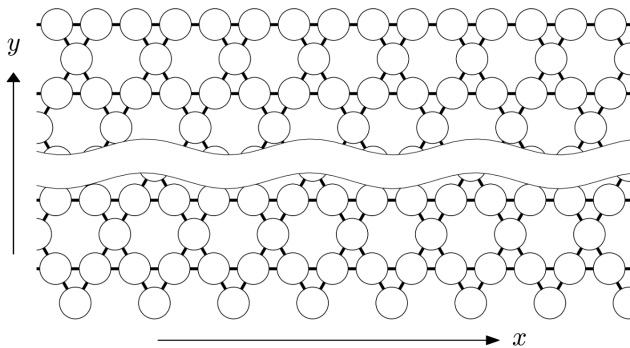


FIG. 3. A strip of kagome lattice. The strip is infinite along  $x$  but has a finite extent along  $y$  axis. The upper and lower boundaries are cut differently to study the effect of boundaries on the propagation of the topological edge modes.

$$\hat{H}_{\mathbf{q}} = \frac{\sqrt{3}}{2} \left[ (q_x + \sqrt{3}q_y) \hat{\sigma}_z \otimes \hat{\sigma}_z + (\sqrt{3}q_x - q_y) \hat{\sigma}_x \otimes \hat{\sigma}_0 \right] + \frac{3\delta J}{4} (\hat{\sigma}_0 + \hat{\sigma}_y) \otimes \boldsymbol{\sigma} \cdot \mathbf{q}, \quad (9)$$

and the effective spin-orbit Hamiltonian

$$\hat{H}_{\mathbf{q}}^{SO} = (\hat{\sigma}_0 + \hat{\sigma}_y) \otimes \hat{H}_R + \hat{\sigma}_x \otimes \hat{H}_D, \quad (10)$$

containing Rashba

$$\hat{H}_R = \frac{\delta J \sqrt{3}}{4} (q_y \hat{\sigma}_x - q_x \hat{\sigma}_y), \quad (11)$$

and Dresselhaus

$$\hat{H}_D = \frac{\delta J \sqrt{3}}{2} (-q_x \hat{\sigma}_x + q_y \hat{\sigma}_y) \quad (12)$$

spin-orbit interaction terms. At the very Dirac point ( $\mathbf{q} = 0$ ) the four eigenenergies of the Hamiltonian (7) are those of the Hamiltonian (8), which are  $E = \pm\Omega$ ,  $\pm\sqrt{4\delta J^2 + \Omega^2}$  measured relative to the energy of the Dirac point at  $\delta J = 0$ ,  $\Omega = 0$ .

### III. TOPOLOGY OF BLOCH BANDS

Topological ideas have become ubiquitous in condensed matter physics<sup>39–41</sup> over the past few decades since the seminal work of Berry<sup>42</sup> in which he demonstrated that the wave function of any quantum system gains an extra phase, Berry phase, (which sometimes is also called Pancharatnam–Berry phase, see preceding work<sup>43</sup>) during adiabatic evolution around a closed path in momentum space. One of the most striking consequences of Berry phase is a dramatic modification of semiclassical equation of motion, that describes a response to a quasi-uniform field which is homogeneous

on the scale of a unit cell. The Berry curvature is analogous to magnetic field and contributes the term known as anomalous velocity to the quasiclassical equation of motion of an electron<sup>44</sup>. Thus, Berry curvature restores the complete symmetry between real and reciprocal spaces with anomalous velocity term which represents the current that flows within the unit cell as the charge is redistributed between the orbitals as quasimomentum changes.

It turns out that the appearance of Berry phase has a profound impact on properties of crystalline solids (see, e.g. Ref.45). In fact, for non-interacting systems the eigenstates respect the periodicity of the Hamiltonian, so that the corresponding Brillouin zone can be considered as a parameter space of the Hamiltonian determined by the quasimomentum. Thus, during evolution in quasimomentum space the underlying Bloch state picks up a phase shift which appears to be gauge-independent if the trajectory is closed. In the meanwhile, the Brillouin zone is isomorphic to a torus, i.e., quasimomenta differ by a reciprocal lattice vector are to be identified.

To analyze topology of polaritonic Bloch bands it is enough to study the bands either below or above the gap of interest. This is because topology of the whole Bloch bundle is trivial (see, e.g. review 46) and, therefore, each of the two parts reflects topology of the other. Chern number of the bands  $C$  below the gap  $E_g$  is given by

$$C = \sum_{E_m < E_g} C_m = \frac{1}{2\pi} \sum_{E_m < E_g} \iint_{BZ} B_{\mathbf{k},m} d^2\mathbf{k}, \quad (13)$$

where the Berry curvature for the  $m$ th band is

$$B_{\mathbf{k},m} = -2 \text{Im} \left\langle \frac{\partial}{\partial k_x} u_{\mathbf{k},m}, \frac{\partial}{\partial k_y} u_{\mathbf{k},m} \right\rangle. \quad (14)$$

Integrating the Berry curvature over the Brillouin zone for the bands below/above the gap  $E_g = -1$  on Fig. 2b yields the Chern numbers  $C = \pm 2$ . According to the bulk-boundary correspondence, a non-zero difference in Chern numbers of the bands across the gap necessarily leads to existence of edge states localized along the boundary.

Such edge states are direct analogs of electronic edge modes of arising in topological insulators. While the electronic band structure of a topological insulator is gapped in the bulk, it allows travelling of gapless edge states that are topologically protected against inhomogeneities and variation of the material parameters.

### IV. EDGE STATES

To study the edge states indicated by the non-trivial topology of the Bloch bands we consider a strip of kagome lattice which is infinite along  $x$  and has a finite extent of  $N_y = 30$  unit cells along  $y$ , see Fig. 3. We intentionally choose different boundary conditions at the upper and lower edge in order to study the effect of the boundaries

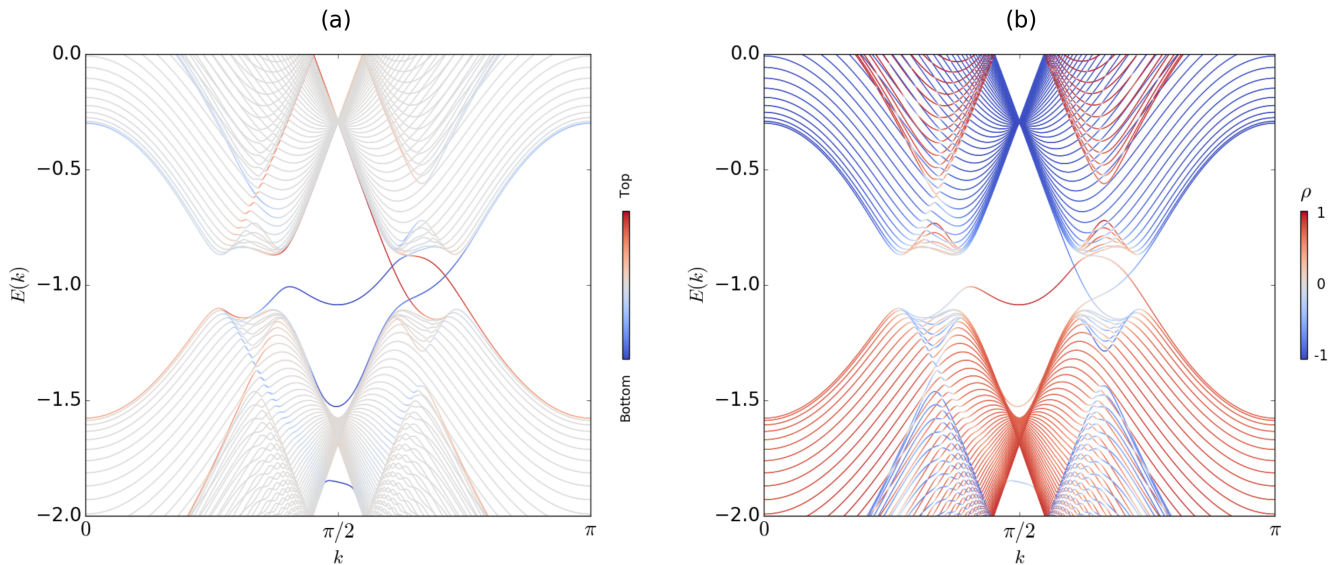


FIG. 4. (Color online) Band structure for the strip of kagome lattice shown on Fig. 3 at  $\delta J = 0.15$ ,  $\Omega = 0.3$ . For convenience, the shifted Brillouin zone is used for better representation of the edge state dispersions. The color scale in (a) encodes localization of the eigenstates defined by the formula (15) where linear weight function was used. Red and blue color correspond to the states localized on the upper and lower boundaries of the strip, respectively, see Fig. 3. The color scale in (b) represents the polarization degree given by the Eq. (16). Band inversion can be seen in the areas above and below the gap where the red and blue lines mix.

on the dispersions of the edge modes. The dispersion of the strip modes is presented in Fig. 4a, as a function of momentum  $k$  along the  $x$  direction. We use the shifted Brillouin zone with  $k$  in the range  $[0, \pi)$  for a better display of the edge state dispersions. In accordance with calculation of the Chern numbers there emerge 4 edge states whose energies lie inside the gap.

To study localization of the eigenstates on the boundaries we define a quantity describing localization of a state  $u_{k,m}^\sigma$  by forming a convolution with the weight function  $p(y)$ ,

$$\lambda_m(k) = \sum_{\sigma,j} p(y_j) |u_{k,m}^\sigma(y_j)|^2, \quad (15)$$

where  $y_j$  are positions of the cells along the  $y$  axis. To obtain results presented in the Fig. 4a we used a linear localization weight function  $p(y) \sim y - \frac{1}{2}\Delta y$ , where  $\Delta y$  is the width of the strip. As seen from the Fig. 4a, there are four dispersion relations which connect topologically non-trivial polaritonic Bloch bundles. These correspond to the topological edge states localized on the two boundaries. The influence of different boundary conditions can be traced by noticing the asymmetry of the dispersions with respect to inversion of the quasimomentum  $k \rightarrow -k$  (i.e. with respect to  $k = \pi/2$  point for the shifted Brillouin zone on Fig. 4).

The remarkable feature arising at the chosen set of parameters ( $\delta J = 0.15$  and  $\Omega = 0.3$ ) is that at a fixed energy there exist more than two edge modes. For the case of the lower boundary in Fig. 3 on of the edge dispersion

relation is not a monotonous function. Thus, at the energy in the interval between the minimum and maximum there appear a pair of additional edge modes with opposite group velocities. This makes polaritonic Kagome lattice qualitatively different from the case of polariton graphene studied in the Ref. 29. Such situation indicates that the number of the edge nodes observed at a given energy may not be equal to the difference of topological invariants connecting the two bands such as the Chern numbers, but be larger by an even number due to appearance of the additional pair of topological edge modes. Because changing the boundary conditions may both create and eliminate the pair of edge states (compare the dispersion of edge states localized on the lower and upper boundary in Fig. 4), creation and annihilation of pairs of edge states are not bound by the topological protection, rather the topological protection only applied to the class of edge states originating from the same dispersion relation which connects topologically nontrivial Bloch bands.

We then study polarization properties of edge states. For the  $m$ -th band we define the degree of polarization,

$$\rho_m(k) = \frac{N_{k,m}^\sigma - N_{k,m}^{\bar{\sigma}}}{N_{k,m}^\sigma + N_{k,m}^{\bar{\sigma}}}, \quad N_{k,m}^\sigma = \sum_j |u_{k,m}^\sigma(y_j)|^2 \quad (16)$$

The band diagram colored by polarization properties allows to see clearly the band inversion in the areas of the energy dispersion where the red and blue curves corresponding to the two polarizations overlap, see Fig. 4b.



Such band inversion is responsible for the appearance of the topological non-trivial phase of polaritonic states.

## V. CONCLUSIONS

We analyzed topological properties of the system of microcavity pillars arranged into a kagome lattice and find that the effective spin-orbit interaction induced by the TE-TM splitting leads to opening of gap in the dispersion in presence of magnetic field. Analysis of the topology of the Bloch bands reveals non-zero Chern numbers and indicate the presence of topologically protected edge states with energies lying inside the gap. We have shown that there exist topological edge states with non-monotonous energy dispersion which leads to the emergence of an additional pair of edge states in the range of energies between the minimum and maximum of the edge state dispersion. We expect that such peculiar shape of dispersion

may be of interest in studies of essentially nonlinear effects such as propagation of edge solitons in polaritonic lattices.

## ACKNOWLEDGMENTS

We acknowledge support of the Ministry of Education and Science of the Russian Federation in the framework of Increase Competitiveness Program 5-100 and of Singaporean Ministry of Education under AcRF Tier 2 grant MOE2015-T2-1-055. D.Y. acknowledges support from RFBR project 16-32-60040. I.V.I. appreciates the support of the Ministry of Education and Science of the Russian Federation (Zadanie No. 3.1231.2014/K), Grant of the President of Russian Federation (MK-5220.2015.2) and RFBR project 16-32-60123. I.V.I. and I.A.S. thank the support from Rannis excellence grant 163082-051.

- 
- \* d.r.gulevich@lmc.ifmo.ru
- <sup>1</sup> L. D. Landau and E. M. Lifshitz. *Statistical Physics: Volume 5 (Course of Theoretical Physics)*, Butterworth-Heinemann, 1980.
  - <sup>2</sup> R. E. Prange and S. M. Girvin. *The Quantum Hall Effect* (Springer-Verlag, New York, 1990).
  - <sup>3</sup> X.-G. Wen, Phys. Rev. B **40**, 7387 (1989).
  - <sup>4</sup> X.-G. Wen, Int. J. Mod. Phys **B4**, 239 (1990).
  - <sup>5</sup> R. Karplus and J.M. Luttinger, Phys. Rev. **95**, 1154 (1954).
  - <sup>6</sup> G. Sundaram and Q. Niu, Phys. Rev. B **59**, 14915 (1999).
  - <sup>7</sup> X.-G. Wen, Adv. Phys. **44**, 405 (1995).
  - <sup>8</sup> C. L. Kane and E. J. Mele, Phys. Rev. Lett. **95**, 226801 (2005); *ibid.* **95**, 146802 (2005).
  - <sup>9</sup> B. A. Bernevig, T. L. Hughes, and S. C. Zhang, Science **314**, 1757 (2006).
  - <sup>10</sup> M. König, S. Wiedmann, C. Brüne, A. Roth, H. Buhmann, L. W. Molenkamp, X.-L. Qi, S.-C. Zhang, Science **318**, 766 (2007).
  - <sup>11</sup> D. Hsieh, D. Qian, L. Wray, Y. Xia, Y. S. Hor, R. J. Cava, and M. Z. Hasan, Nature **452**, 970 (2008).
  - <sup>12</sup> F. Haldane, and S. Raghu, Phys. Rev. Lett. **100**, 013904 (2008).
  - <sup>13</sup> A.B. Khanikaev, S.H. Mousavi, W.-K. Tse, M. Kargarian, A.H. MacDonald, and G. Shvets, Nature Materials **12**, 233-239 (2013).
  - <sup>14</sup> Z. Wang, Y. Chong, J.D. Joannopoulos, and Marin Soljacic, Nature **461**, 772-775 (2009).
  - <sup>15</sup> I. Carusotto and C. Ciuti, Rev. Mod. Phys. **85**, 299 (2013).
  - <sup>16</sup> J. Kasprzak, et al., Nature **443**, 409 (2006).
  - <sup>17</sup> H. Deng, H. Haug, and Y. Yamamoto, Rev. Mod. Phys. **82**, 1489 (2010).
  - <sup>18</sup> A. Imamoglu, R. J. Ram, S. Pau, and Y. Yamamoto, Phys. Rev. A **53**, 4250 (1996).
  - <sup>19</sup> H. Deng, G. Weihs, D. Snoke, J. Bloch, and Y. Yamamoto, Proc. Natl. Acad. Sci. **100**, 15318 (2003).
  - <sup>20</sup> E. A. Cerda-Méndez et al., Phys. Rev. B **86**, 100301 (2012).
  - <sup>21</sup> E. A. Cerda-Méndez, Phys. Rev. Lett. **105**, 116402 (2010).
  - <sup>22</sup> N. Y. Kim, K. Kusudo, C. Wu, N. Masumoto, A. Lffler, S. Hfling, N. Kumada, L. Worschech, A. Forchel, and Y. Yamamoto, Nat. Phys. **7**, 681 (2011).
  - <sup>23</sup> N. Masumoto et al., New J. Phys. **14**, 065002 (2012).
  - <sup>24</sup> N. Y. Kim, K. Kusudo, A. Lffler, S. Hfling, A. Forchel, and Y. Yamamoto, New J. Phys. **15**, 035032 (2013).
  - <sup>25</sup> K. Kusudo, N. Y. Kim, A. Lffler, S. Hfling, A. Forchel, and Y. Yamamoto, Phys. Rev. B **87**, 214503 (2013).
  - <sup>26</sup> T. Jacqmin et al. Phys. Rev. Lett. **112**, 116402 (2014).
  - <sup>27</sup> M. Milićević et al., 2D Mater. **2**, 034012 (2015).
  - <sup>28</sup> V. G. Sala et al., Phys. Rev. X **5**, 011034 (2015).
  - <sup>29</sup> A. V. Nalitov, G. Malpuech, H. Terças, and D. D. Solnyshkov, Phys. Rev. Lett. **114**, 026803 (2015).
  - <sup>30</sup> A. Kuther et al., Phys. Rev. B **58**, 15744 (1998).
  - <sup>31</sup> G. Panzarini et al., Phys. Rev. B **59**, 5082 (1999).
  - <sup>32</sup> G. Dasbach et al., Phys. Rev. B **71**, 161308(R) (2005).
  - <sup>33</sup> A. V. Nalitov, D. D. Solnyshkov, and G. Malpuech, Phys. Rev. Lett. **114**, 116401 (2015).
  - <sup>34</sup> T. Karzig, C.-E. Bardyn, N. H. Lindner and G. Refael, Phys. Rev. X **5**, 031001 (2015).
  - <sup>35</sup> C.-E. Bardyn, T. Karzig, G. Refael and T. C. H. Liew, Phys. Rev. B **91**, 161413 (2015).
  - <sup>36</sup> M. Mekata Phys. Today **56**, 12 (2003).
  - <sup>37</sup> M. Pereiro et al., Nat. Comm. **5**, 4815 (2014).
  - <sup>38</sup> R. Chisnell et al., Phys. Rev. Lett. **115**, 147201 (2015).
  - <sup>39</sup> A. S. Schwarz, *Quantum Field Theory and Topology*, Springer-Verlag, Berlin, 1993.
  - <sup>40</sup> M. Monastyrsky, *Topology of Gauge Fields and Condensed Matter*, Springer, New York, 1993.
  - <sup>41</sup> M. Nakahara, *Geometry, Topology and Physics*, Taylor & Francis Group, New York, 2003.
  - <sup>42</sup> M. V. Berry, Proc. R. Soc. London Ser. A **392**, 45 (1984).
  - <sup>43</sup> S. Pancharatnam, Proceedings of the Indian Academy of Science A **44**, 247 (1956).
  - <sup>44</sup> G. Sundaram and Q. Niu, Phys. Rev. B **59**, 14915 (1999).
  - <sup>45</sup> D. Xiao, M.-C. Chang, and Q. Niu, Rev. Mod. Phys. **82**, 1959 (2010).
  - <sup>46</sup> M. Fruchart and D. Carpentier, C. R. Physique **14** (2013) 779.